Adaptive-Predictive Control of Kamyr Digester Chip Level

Kamyr digester chip level poses a difficult control problem, because the chip column dynamics are complex and it is difficult to measure the chip-liquor interface. Control of the chip level is required to smooth digester operation and to stabilize the residence time. Conventional methods rely largely on fixed parameter controllers which are unable to compensate for changes in the process dynamics. Manual controller retuning is often required.

An adaptive chip level controller based on Generalized Predictive Control (GPC) is presented. Closed-loop time series identification methods were used to develop the process model and to design the controller. A significant reduction in chip level and P-number variability has been observed since commissioning the controller on an industrial digester in September 1988. The adaptive controller has eliminated the need for manual retuning, reduced the need for operator intervention, and demonstrated the potential to predict hang-ups.

Bruce J. Allison
Guy A. Dumont
Pulp and Paper Research Institute of Canada
Control Engineering Section
Vancouver, BC, Canada V6S 2L9

Lloyd H. Novak
William J. Cheetham
MacMillan Bloedel Ltd.
Alberni Pulp and Paper Division
Port Alberni, BC, Canada V9Y 5J7

Introduction

An important problem in the production of chemical pulps from continuous Kamyr digesters is the control of wood chip level. The chip level determines the residence time and, therefore, the extent of reaction (Vroom, 1957). Chip level is difficult to control for two reasons. First, the measurement is difficult because the chip level is generally below the liquor level. Strain gauges are used predominantly but are characterized by poor resolution and extremely high measurement noise. Second, changes in chip size, density, species, and moisture content all affect the packing of chips in the digester and the movement of the chip column. This results in time and operating point dependent changes in the process dynamics. A controller for this problem must therefore be capable of handling noisy data and must be robust to modeling errors.

Self-tuning regulators have long been considered an ideal solution to these types of control problems. Dumont (1986) reviewed adaptive control applications in the pulp and paper industry. Self-tuners have been applied to Kamyr digester chip level by Cegrell and Hedqvist (1974), Sastry (1978), and Bélanger et al. (1986). Not much information is available about the first study and the second was finally abandoned. However, the third application has been working successfully on an industrial digester since 1983. This generalized minimum-variance (GMV) controller (Clarke and Gawthrop, 1975) uses top separator motor load as the chip level measurement. The problem with this strategy is that many mills are reluctant to operate with the chip level up in the top separator for fear of overloading the top separator motor or of losing the chip level entirely. Moreover, the GMV controller can perform poorly if the process deadtime is incorrectly specified or changes with time.

In this paper we present the design and industrial application of an adaptive controller based on generalized predictive control (GPC) (Clarke et al., 1987a,b) and on the use of strain gauge level measurements. GPC is based on on-line estimation of an explicit process model and solution of a predictive controller design problem. Closed-loop time series identification methods were used to develop the model and to design the controller. An advantage of using an explicit model is that fewer parameters need to be identified on-line than with equivalent implicit schemes. Furthermore, the parameters of explicit models are more readily identified with physically significant parts of the system and, therefore, provide more insight into the process. The predictive control law provides robustness to modeling errors and gives the engineer a simple performance-related tuning

Correspondence concerning this paper should be addressed to B. J. Allison.
G. A. Dumont is now with the Department of Electrical Engineering, University of British Columbia.

parameter that is directly related to the desired closed-loop settling time. The resulting strategy has been operating successfully on an industrial digester since September, 1988. The benefits include a reduction in chip level variability and a more uniform pulp. The adaptive control strategy has also demonstrated the potential to detect hang-ups, a common fault in digester operation.

Process Description

Kraft pulping involves the chemical breakdown of wood chips into individual fibers by the addition of a liquor composed of sodium hydroxide and sodium sulfide. The cooking reaction typically requires heating the reactants to 170°C for 3 h to dissolve the lignin that binds the fibers together. Cooking takes place in either batch or continuous reactors called digesters. The extent of reaction is related to both temperature and time through an Arrhenius-type equation (Vroom, 1957). The principal features of a Kamyr digester are shown in Figure 1. The production rate is determined by the chip meter, which feeds wood chips to the steaming tube. The primary purpose of steaming the chips is to drive off noncondensable gases and thereby aid liquor impregnation. After steaming, the chips are mixed with circulating liquor in the high-pressure feeder and fed to the digester through the top separator. The top separator basically consists of a screw conveyor that pushes the chips downward into the digester. The chip–liquor mass passes through three distinct zones: impregnation, cooking, and washing. The impregnation zone allows the liquor to diffuse into the chips. Heat is added in the cooking zone and delignification starts. The reaction is stopped by the countercurrent flow of cooler spent liquor from the wash zone. The total residence time is on the order of 5 h. The rate of pulp removal is controlled by manipulating the blow flow at the digester bottom.

Chip level measurement is accomplished by a set of three strain gauges spaced about 2 m apart. Each gauge consists of a blade located at right angles to the digester wall and attached to a torque measuring device. A continuous signal roughly proportional to the momentum of the chip column is generated, but the signals are extremely noisy because of the heterogeneity of the column. In most modern control systems, signals from the individual gauges are combined to calculate a single composite level measurement. The extremely poor resolution of the signal complicates the design and tuning of traditional process control strategies and has prompted the development of many heuristic level control schemes (Cohen and Ryan, 1974).

Blow flow, bottom scraper speed, and chip meter speed have all been used to control chip level. Lindqvist (1982), for example, used the chip meter and blow flow in a split-range configuration: the chip meter speed was changed for small variations and the blow flow for large. In another application, Bélanger et al. (1986) observed little difference between using the blow flow and the outlet device as the final control element.

The industrial digester under study in this application produces 350 tpd (tons per day) of kraft pulp. Basically two grades are manufactured, one consisting of 100% hemlock and the other consisting of a hemlock-cedar mix. The control system consists of a DEC PDP 11/73 computer implementing a MoDo Chemetics control strategy and playing host to a Honeywell TDC 2000. The composite chip level signal is calculated from the three strain gauges using a proprietary scheme developed by MoDo. The top separator motor load is used to indicate high level conditions. Prior to implementing our adaptive control

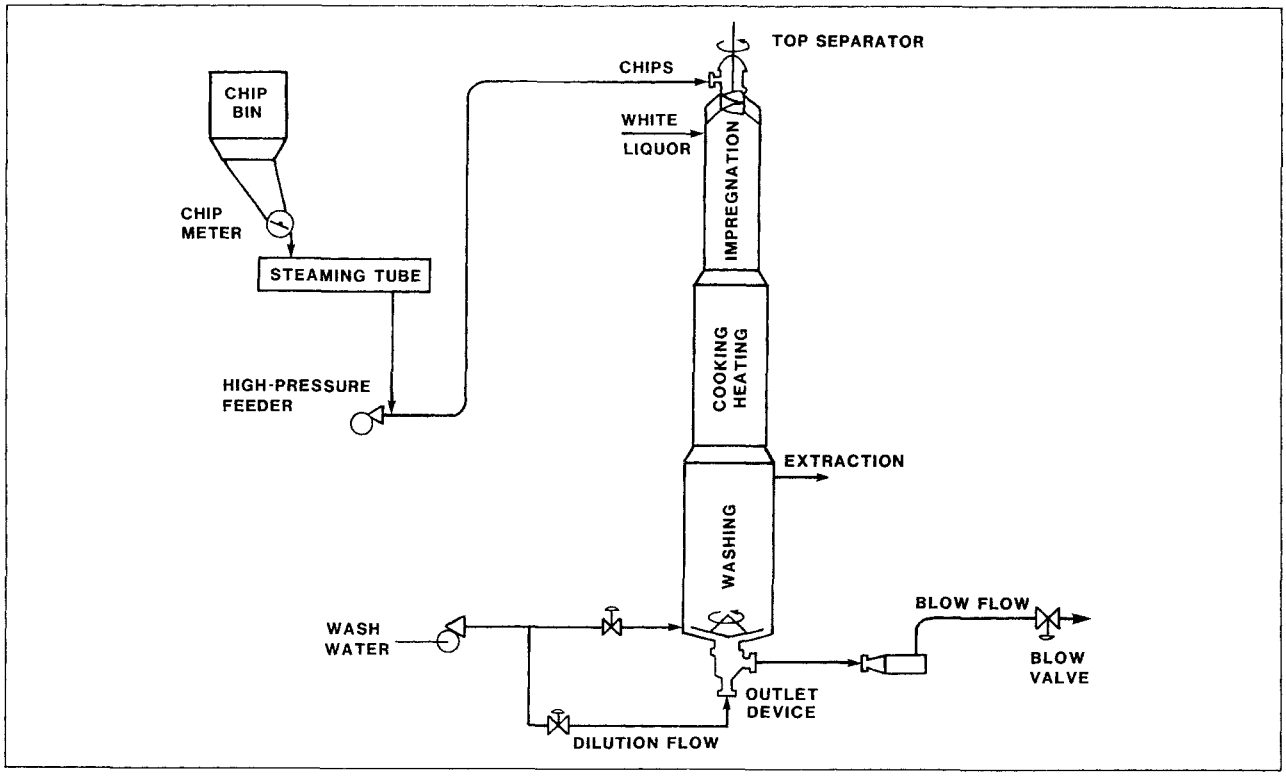

Figure 1. Kamyr digester.

strategy, a discrete proportional integral derivative (PID) controller, implemented in the host, regulated the chip level by manipulating the blow flow setpoint, Figure 2. An additional proportional-only feedback from top separator motor load was used in the event of high motor amperage. The strategy also included steady-state feedforward control for production rate changes. The control interval was 30 s. The main problem was with the PID controller. It had to be detuned because of uncertainty in the process dynamics and noise in the level signal. Furthermore, the integral term was almost completely eliminated and, therefore, the controller could not compensate for persistent offsets, Figure 3.

Process Identification

The complexity of a first principles approach to process modeling led us to use input/output models, derived experimentally. In the design of advanced model-based controllers, the sampling interval is an important design parameter. Generally, as the sampling interval is decreased the control performance will improve, but at the expense of greater control effort. However, in the case of adaptive control, controlling and updating too rapidly can have an adverse effect, usually resulting in the need to estimate more parameters. Therefore, a compromise must always be struck between a small sampling interval for good control and a larger sampling interval for parameter estimation. Åström and Wittenmark (1989) suggest sampling 5–20 times over an open-loop step response. Bélanger et al. (1986) identified the dominant process time constant in their study to be 40 min. In light of this information and an unsuccessful attempt to identify the process using a 2 min sampling interval, a 5 min sampling interval was chosen. Note, however, that the raw level signal is still computed and digitally filtered once every 30 s.

For safety, and because of tight product specifications, data for model building must often be obtained during closed-loop operation in which a feedback controller attempts to eliminate at least major deviations of the process output from target. The difficulty of conducting process identification in closed-loop operation is that the input is no longer independent of the disturbances affecting the output. Therefore, it is often necessary to temporarily add an additional, artificially generated noise source sometimes called a dither signal, Figure 4, to the input which is uncorrelated with the disturbances.

Figure 5 shows digester chip level and blow flow setpoint data collected when the process was under proportional-only feedback control and a dither signal was added to the blow flow setpoint. Two hundred and eighty-seven (287) observations were collected at 5 min intervals over a period of one day. The dither signal in this case was a pseudorandom binary sequence (PRBS)

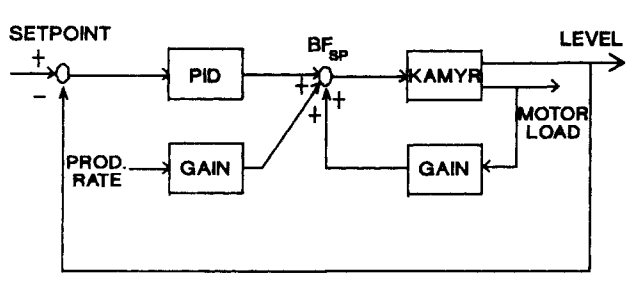

Figure 2. Conventional chip level control strategy.

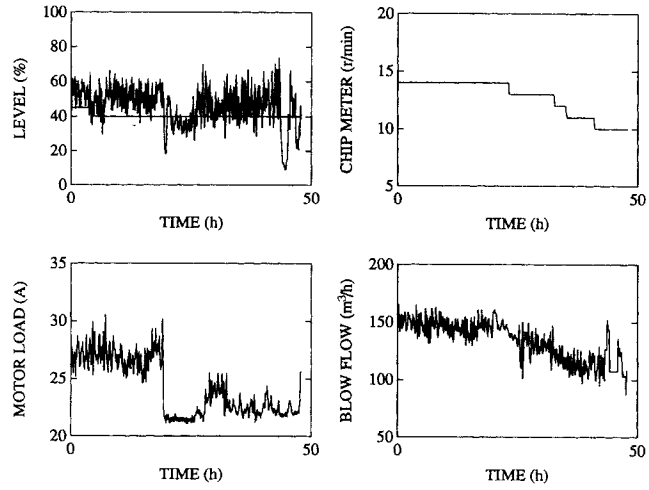

Figure 3. Conventional control.

of ±10 m³/h and was added to the blow flow setpoint. Each time a new blow flow setpoint was calculated by the feedback controller, a random number generator in the host computer was used to simulate the flip of a coin to decide if a switch in the dither signal was required. Although no change in grade occurred during the data collection period, two production rate changes occurred, the first a decrease from 16 to 14 rpm at t = 3.5 h and the second an increase from 14 to 17 rpm at t = 11.5 h. Note that the process was reasonably well controlled despite the addition of the dither signal.

The data shown in Figure 5 were analyzed using methods suggested by Box and MacGregor (1974). Consider a process described by the linear transfer function plus noise model (Box and Jenkins, 1976):

$$Y_t = \frac{\omega(z^{-1})}{\delta(z^{-1})} U_{t-f-1} + N_t$$

$$N_t = \frac{\theta(z^{-1})}{\phi(z^{-1})\nabla^d} a_t \qquad (1)$$

This dynamic-stochastic transfer function form is often referred to as the additive form because the deterministic transfer function and stochastic noise model components are kept separate. In the model, Eq. 1, Y_t is the output deviation from its target value at time t and U_t is the input deviation from a corresponding steady-state value. The terms $\omega(z^{-1})$ and $\delta(z^{-1})$

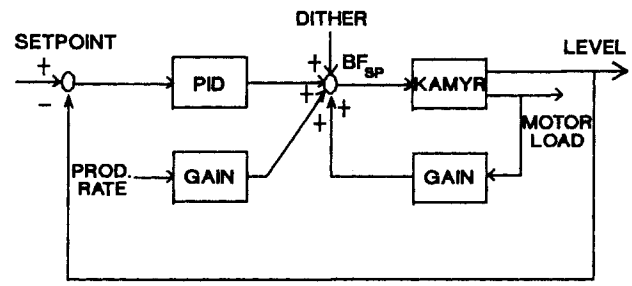

Figure 4. Control configuration during identification experiment.

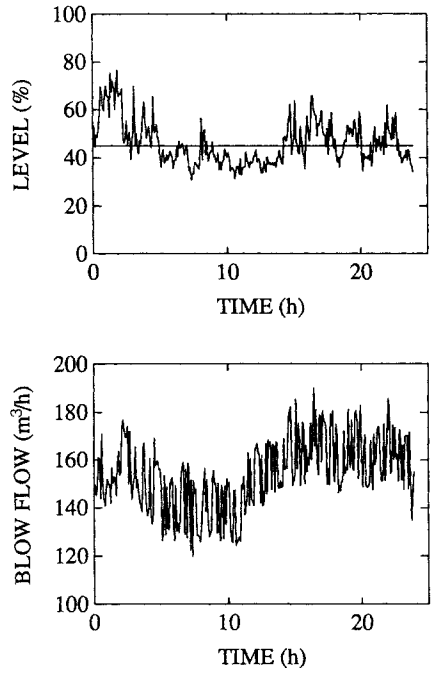

Figure 5. Data for model identification.

in the deterministic transfer function are polynomials in the backward shift operator z^{-1} ($z^{-1}Y_t = Y_{t-1}$). The parameter f (≥ 0) is the number of whole sampling intervals of pure process delay. One additional period of delay is introduced by the sample and hold operation of the computer. The stochastic disturbance N_t represents the joint effect at the output of all unobserved disturbances acting within the system. In the absence of some compensating action, these disturbances lead to output deviations from target. The disturbances may be modeled by passing an independent, normally distributed (white) noise sequence a_t with variance σ_a^2 through a linear dynamic transfer function. In the autoregressive integrated moving-average (ARIMA) noise model, $\theta(z^{-1})$ is a polynomial with all roots lying inside the unit circle (in the z plane). $\phi(z^{-1})\nabla^d$ is a polynomial with d roots equal to unity. ∇ is the backward difference operator, $\nabla = (1 - z^{-1})$. The allowance of d roots equal to unity ($d = 0$ or 1 usually) enables one to characterize the type of nonstationary drifting behavior that process variables tend to exhibit when uncontrolled. As we shall see, this naturally leads to integral action in the controller.

In order to identify the input/output transfer function model orders from the data shown in Figure 5, the following expression, which relates the crosscovariances between the dither signal and the input $\gamma_{du}(k)$ and the dither signal and the output $\gamma_{dy}(k)$, was used to obtain an estimate of the process impulse weights $\hat{\nu}_i$ (Box and MacGregor, 1974):

$$\gamma_{dy}(k) = \nu_0\gamma_{du}(k) + \nu_1\gamma_{du}(k-1) + \cdots \qquad k \geq 0 \qquad (2)$$

Assuming that the ν_i weights are effectively zero beyond $k = K$, and substituting estimates for the two sets of crosscovariances, the first $K + 1$ equations are solved for $\hat{\nu}_i$, $i = 0, 1, \ldots, K$. The impulse weights give an estimate of the response of the process output to a unit impulse disturbance occurring in the input.

Figure 6 shows the impulse weights estimated using the chip

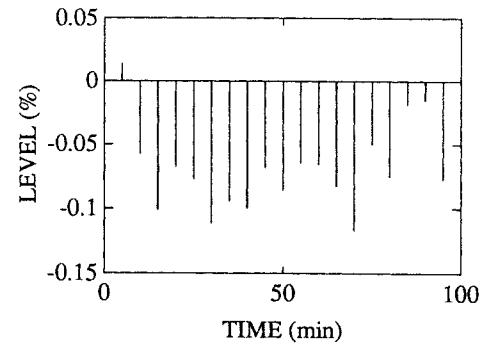

Figure 6. Estimated process impulse response.

level/blow flow data from Figure 5. The first impulse weight is small in magnitude and of the wrong sign. An increase in blow flow should cause a decrease in chip level. Therefore, this first impulse weight is deemed insignificant, indicating that the process has one complete sampling interval (5 min) of pure delay ($f = 1$). This delay may be attributed to the finite time required to accelerate the chip column because of its elastic characteristics (Cegrell and Hedqvist, 1974). The remaining impulse weights suggest one of several alternatives for the orders of the transfer function polynomials $\omega(z^{-1})$ and $\delta(z^{-1})$. The two most likely alternatives are first order with fractional delay, or second order.

The step response, Figure 7, obtained by integrating the impulse weights in Figure 6, may be used as an additional check on the transfer function delay and to give an estimate of the gain and time constant. A visual extrapolation of the step response appears to indicate that the process has an approximate first-order time constant of 65 min and steady-state gain of $-1.5\% \cdot \text{h/m}^3$. These estimates were used as initial guesses in the fitting stage.

An iterative model-building procedure consisting of structure identification, fitting, and diagnostic checking stages identified the following dynamic-stochastic model structure:

$$Y_t = \frac{\omega_0}{1 - \delta_1 z^{-1}} U_{t-2} + \frac{1 - \theta_1 z^{-1}}{\nabla} a_t \qquad (3)$$

Fitting this model to the data gave the following parameter estimates:

$$Y_t = \frac{-0.076}{1 - 0.91z^{-1}} U_{t-2} + \frac{1 - 0.50z^{-1}}{\nabla} a_t, \quad \sigma_a^2 = 31 \qquad (4)$$

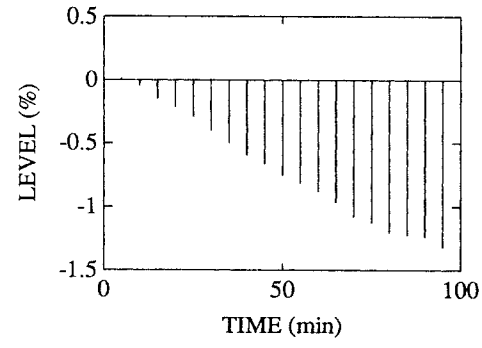

Figure 7. Estimated process step response.

The first term in Eq. 4 indicates that the level responds as a first-order plus deadtime process, with a gain of $-0.89\% \cdot h/m^3$ and a time constant of 56 min. Note that these values are close to the rough estimates obtained earlier from the step response, Figure 7. The second term in Eq. 4 is the stochastic noise model, which characterizes the combined effect of all disturbances and measurement noise on the output. The noise model structure in this case is integrated moving-average IMA(1, 1). This indicates that the chip level exhibits a drifting type of nonstationary behavior buried in measurement noise. This disturbance model structure is common in the process industries.

Some discussion of an apparent inconsistency in the process model, Eq. 4, is appropriate at this point. We know from a simple process mass balance (Fuchs and Smith, 1971) that the process is an integrator, that is, theoretically $\delta(z^{-1}) = 1 - z^{-1}$. However, our identification experiment indicates that the process is first order, albeit with a fairly lengthy time constant. The identified discrete time constant $\delta_1 = 0.91$ is a low estimate of the true process time constant because the switching time used during the identification experiment was faster than ideal. Ideally, the input sequence during identification should excite frequencies around the breakpoint frequency of the process. An integrator has an infinitely low breakpoint frequency (its Bode plot continually decreases with increasing frequency), which dictates using a very slow switching time. We chose to switch more frequently (once every sample time) because we wanted to minimize the effect of the dither signal on the output. We were also more interested in estimating the transient characteristics of the process (the deadtime and model orders) as opposed to steady-state effects. Some of the controller design implications of this discrepancy are discussed in the following section.

Design of the Adaptive Controller

Adaptive control is based on the separation theorem or the certainty equivalence principle. This implies that the optimal control strategy can be separated into two parts:

1. a parameter estimator
2. a predictive controller

It should be noted that the resulting control strategy is optimal only in the sense that it minimizes a certain performance criterion (usually a weighted sum of the input and output variances) and not in any overall sense as the name may tend to imply.

It is well known that the success of many industrial adaptive control applications comes from building as much a priori process knowledge into the algorithm as possible. This section describes how we used prior knowledge to make many of the engineering decisions that were involved in designing the parameter estimator and the predictive controller.

Combined form of the process model

When considering on-line parameter estimation, such as in adaptive control, the combined difference equation structure offers considerable advantages over the additive form. In this representation the effects of the process input and stochastic disturbances are combined into the single difference equation model:

$$A(z^{-1})\nabla^d Y_t = B(z^{-1})\nabla^d U_{t-f-1} + C(z^{-1})a_t \qquad (5)$$

The additive model may be placed in the combined form by multiplying both sides of Eq. 3 by the denominators of the righthand side terms to give:

$$(1 - \delta_1 z^{-1})\nabla Y_t = \omega_0 \nabla U_{t-2} + (1 - (\delta_1 + \theta_1)z^{-1} + \delta_1\theta_1 z^{-2})\, a_t \qquad (6)$$

and then making the following substitutions; $a_1 = \delta_1$, $b_0 = \omega_0$, $c_1 = \delta_1 + \theta_1$ and $c_2 = -\delta_1\theta_1$ to give:

$$(1 - a_1 z^{-1})\nabla Y_t = b_0 \nabla U_{t-2} + (1 - c_1 z^{-1} - c_2 z^{-2})a_t \qquad (7)$$

Note that when placed in the combined form, the additive model parameters appear as nonlinear products, Eq. 6. Therefore, the parameters of the combined form cannot always be identified with physically significant parts of the system. This is why we chose the additive form for our preliminary analysis. The combined form provides less insight than the additive form because the dynamic and stochastic parts of the system are no longer kept as distinct terms but rather are combined into the $A(z^{-1})$, $B(z^{-1})$, and $C(z^{-1})$ terms. However, the combined model form is necessary for adaptive control because the parameters are distinct and, therefore, are easily estimated by recursive estimation algorithms.

Compensating for deadtime changes

The ability to adapt to changes in deadtime comes from estimating a number of trailing coefficients in the B polynomial, Eq. 5. Experience indicates that the deadtime in a chip level control loop may be between 0 and 20 min (Fuchs and Smith, 1971; Sastry, 1978; Bélanger et al., 1986). In this application we felt that because the digester was operating at a high production rate during the identification experiment, the identified deadtime of 10 min was a good estimate of the minimum process delay. Therefore, we allowed the estimator to calculate the deadtime in the range 10 to 20 min. This was accomplished by modifying the model, Eq. 7, to include two trailing coefficients in $B(z^{-1})$:

$$(1 - a_1 z^{-1})\nabla Y_t = (b_0 + b_1 z^{-1} + b_2 z^{-2})\nabla U_{t-2} + (1 - c_1 z^{-1} - c_2 z^{-2})a_t \qquad (8)$$

Our subsequent experience has led us to believe that this is a conservative upper bound, that is, the maximum delay is likely less than 20 min.

Reducing the number of estimated parameters

During implementation of the adaptive controller, we decided to fix the parameters of $A(z^{-1})$ and $C(z^{-1})$, Eq. 8, and only estimate $B(z^{-1})$ on-line. Fixing the parameters of $A(z^{-1})$ and $C(z^{-1})$ inhibits the algorithm from compensating for changes in the process time constant and disturbance characteristics, while estimating an expanded B polynomial provides the capability of compensating for changes in the process gain and deadtime. This is due to the fact that fixing $A(z^{-1})$ and $C(z^{-1})$ in Eq. 8 is equivalent to fixing $\delta(z^{-1})$ and $\theta(z^{-1})$ in the additive model, Eq. 3. The following discussion justifies this decision, with reference to the additive model.

The moving-average polynomial $\theta(z^{-1}) = (1 - \theta_1 z^{-1})$ in Eq. 3 contains the stationary component of the disturbance model.

Several checks were made on the value of the moving-average parameter θ_1 by refitting the model to closed-loop data sets obtained during normal operation. The identified θ_1 values were consistently in the range $0.45 \leq \theta_1 \leq 0.50$. The value $\theta_1 = 0.5$ was finally chosen for implementation because this was the more conservative choice. This has to do with the role which the θ polynomial plays as a low-pass filter for the measurement in constrained minimum variance controllers (Bergh and MacGregor, 1987).

The δ polynomial $\delta(z^{-1}) = (1 - \delta_1 z^{-1})$ in Eq. 3 contains the pole of the input/output transfer functional model. Theoretically, we know the underlying process to be an integrator, that is, theoretically $\delta_1 = 1.0$. No change in operating point, grade, or any other factor changes this fact. However, because the controller contains an inversion of the process model, forcing an integrator into the model (i.e., $\delta_1 = 1$) would effectively cancel the controller's integral action; this was the problem encountered with the Dahlin controller application investigated by Fuchs and Smith (1971). To see this, an expression was derived for the controller reset time. The integral contribution to a PID controller is usually expressed as a reset time. The rest time is the time required to double the proportional action if no change in the error occurs. For the process given in Eq. 3, GPC has the following reset time (see the Appendix):

$$T_r = \frac{\delta_1}{1 - \delta_1} T \tag{9}$$

where T_r is the reset time and $T = 5$ min is the control interval. The derivation of Eq. 9 is due to Harris et al. (1982), who show that discrete controllers can be separated into terms that represent proportional, integral, first-order, and higher order derivatives, and deadtime compensation contributions. Note that GPC's reset time is determined by the discrete process time constant δ_1 and the control interval T. When δ_1 is small, T_r is small relative to T and the controller contains a large integral contribution. As $\delta_1 \rightarrow 1$, $T_r \rightarrow \infty$ and, in the limit, the controller contains no integral action at all. We felt that at least a small amount of integral action was needed to compensate for input load disturbances and any inaccuracies in the production rate feedforward controller. Simulation results demonstrated that too much integral action could force the system to instability. The problem, therefore, was to find an appropriate value for the parameter δ_1.

Assuming the process to be an integrator, one way of choosing δ_1 is to investigate the penalty associated with deliberately choosing a value less than 1.0 by analyzing its effect on the closed-loop performance. Figure 8 shows the normalized output variance (output variance divided by the residual variance) for a range of δ_1 values between 0.9 and 1.0 and for five different values of the tuning parameter $N2$ (this controller tuning parameter is discussed later). Note that, for $N2 = 2$, 5, and 10, the output variance increases with decreasing δ_1. However, for $N2 = 15$ and 20 the plot goes through a minimum. Therefore, the best choice of δ_1 is dependent on the tuning parameter $N2$. For large values of $N2$ there is a small output variance reduction associated with misplacing δ_1. However, for small $N2$ the shape of the relationship changes, and there is a significant variance increase associated with the same mismatch. Simulation results indicated that constraints on allowable blow flow manipulation would limit us to operating in the range $10 \leq N2 \leq 15$. Given

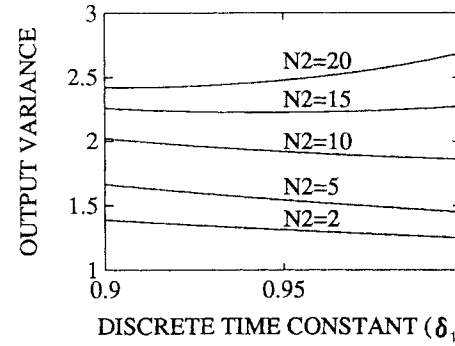

Figure 8. Theoretical performance for different values of discrete time constant δ_1 and tuning parameter $N2$.

that lower values of $N2$ are associated with lower output variances and greater sensitivity to δ_1 mismatch, we chose a fairly conservative value of $\delta_1 = 0.98$. This coincides with a reset time of $T_r = 4$ h, Eq. 9.

Prefiltering the input/output variables

Replacing the A and C polynomials in Eq. 8 by polynomials of constant coefficients (i.e., $a_1 = \delta_1 = 0.98$, $c_1 = \delta_1 + \theta_1 = 1.48$, and $c_2 = -\delta_1 \theta_1 = -0.49$) gives:

$$(1 - 0.98z^{-1})\nabla Y_t = (b_0 + b_1 z^{-1} + b_2 z^{-2})\nabla U_{t-2} + (1 - 1.48z^{-1} + 0.49z^{-2})a_t \tag{10}$$

One advantage of fixing the C polynomial is that the remaining model parameters may be estimated by recursive least squares (RLS). A more advanced estimation algorithm (recursive extended least squares or recursive maximum likelihood) would be required to estimate $C(z^{-1})$ on-line. Dividing both sides of Eq. 10 by $C(z^{-1})$ gives:

$$(1 - 0.98z^{-1})\nabla Y_t^f = (b_0 + b_1 z^{-1} + b_2 z^{-2})\nabla U_{t-2}^f + a_t \tag{11}$$

where superscript f denotes a quantity filtered by $1/C(z^{-1})$. Note that prefiltering the input/output values by $\nabla/C(z^{-1})$ has a band-pass filter effect. The low-pass filter characteristic eliminates high-frequency noise and high-frequency unmodeled components, while the high-pass filter characteristic eliminates low-frequency disturbances and offsets. Note that Eq. 11 may be rearranged to provide an estimate of the differenced and filtered process output at the current sampling instant t:

$$\nabla \hat{Y}_t^f = 0.98\nabla Y_{t-1}^f + b_0 \nabla U_{t-2}^f + b_1 \nabla U_{t-3}^f + b_2 \nabla U_{t-4}^f = \phi_t^T \hat{\theta}_{t-1} \tag{12}$$

where $\phi_t^T = [\nabla Y_{t-1}^f, \nabla U_{t-2}^f, \nabla U_{t-3}^f, \nabla U_{t-4}^f]$ is a regressor vector of past differenced and filtered inputs and outputs and $\hat{\theta}_{t-1} = [0.98, b_0, b_1, b_2]^T$ is a vector of parameter estimates. When the current measurement Y_t becomes available, the prediction error:

$$e_t = \nabla Y_t^f - \phi_t^T \hat{\theta}_{t-1} \tag{13}$$

is calculated and used to update the parameter estimates. The parameter a_1 ($=0.98$) is held constant by zeroing the corresponding row and column in the covariance matrix, as explained later.

Recursive least squares estimator

Conventional recursive least squares (RLS) algorithms based on constant forgetting factor suffer from a problem known as estimator wind-up (Harris et al., 1978; Wittenmark and Åström, 1984) whereby the gain in the parameter updating equation grows without bound when there is not much information in the input/output data. This causes large disturbances in the parameter estimates, which may result in periods of poor control. Periods of little or no input/output information may be caused by saturation of the manipulated variable, large constraints on the control actions, or simply as a result of smooth process operation (i.e., few disturbances or setpoint changes). There are several ways to avoid parameter wind-up. The main idea is to ensure that the covariance matrix P stays bounded. This can be done, for instance, by ensuring that the trace of P is constant at each iteration (Irving, 1979). Another possibility is to adjust the forgetting factor automatically (Fortescue et al., 1981). In this application we implemented the exponential forgetting and resetting algorithm (EFRA) of Salgado et al. (1988). The EFRA employs exponential forgetting of old data to ensure continual parameter adaptation and exponential covariance resetting during periods of low excitation. Simulation studies have shown that the EFRA is superior to the constant trace algorithm and that it guarantees that P remains bounded, something that variable forgetting factor schemes cannot guarantee.

The EFRA is given by:

$$\hat{\theta}_t = \hat{\theta}_{t-1} + \frac{\alpha P_{t-1}\phi_t}{1 + \phi_t^T P_{t-1}\phi_t} e_t \tag{14}$$

$$P_t = \frac{1}{\lambda} P_{t-1} - \frac{\alpha P_{t-1}\phi_t\phi_t^T P_{t-1}}{1 + \phi_t^T P_{t-1}\phi_t} + \beta I - \tau P_{t-1}^2 \tag{15}$$

where α, β, λ, and τ are constants. P_t is a square matrix proportional to the covariance of the parameter estimates. The constants were set to the default values suggested by Salgado et al.: $\alpha = 0.5$ and $\beta = \tau = 0.005$. Note that $\lambda = 0.98$ is the usual forgetting factor. Salgado et al. show that the covariance matrix P_t is bounded:

$$P_{\min} \le P_t \le P_{\max} \quad \text{for all } t \tag{16}$$

where approximate expressions for P_{min} and P_{max} are given by:

$$P_{\min} \approx \frac{\beta}{\alpha - \eta} \tag{17}$$

$$P_{\max} \approx \frac{\eta}{\tau} + \frac{\beta}{\eta} \tag{18}$$

$$\eta \approx \frac{1 - \lambda}{\lambda} \tag{19}$$

Substituting the above constants into Eqs. 19, 17, and 18 gives the following bounds for P_t:

$$0.0104 \le P_t \le 4.33 \quad \text{for all } t \tag{20}$$

Upon start-up, the diagonal elements of P_t were initialized to 1 and the off-diagonal elements to 0.

Generalized predictive control

Generalized predictive control (GPC) (Clarke et al., 1987a,b) is based on the minimization of the following quadratic cost function:

$$J = E\left(\sum_{j=N1}^{N2} [Y_{t+j} - W_{t+j}]^2 + \sum_{j=1}^{NU} \rho[\nabla U_{t+j-1}]^2 \right) \tag{21}$$

where W_{t+j} is a sequence of future setpoints and ρ is a control action weighting factor. In order to perform the minimization future output predictions $\hat{Y}_{t+j}$, $j = N1, N1 + 1, \ldots, N2$ are needed. Note that the independent variables in the minimization are the current control action ∇U_t and $NU - 1$ future control actions ∇U_{t+1}, ∇U_{t+2}, ..., ∇U_{t+NU-1}. In practice, the control actions are recalculated at each control interval and hence only the first (current) control action in the sequence is applied (receding-horizon approach).

To derive a j-step ahead predictor of Y_{t+j} consider the Diophantine identity:

$$C(z^{-1}) = E_j(z^{-1})A(z^{-1})\nabla + z^{-j}F_j(z^{-1}) \tag{22}$$

where $A(z^{-1})$ and $C(z^{-1})$ are polynomials from the combined process model, Eq. 5, and $E_j(z^{-1})$ and $F_j(z^{-1})$ are uniquely defined polynomials in z^{-1}. Note, in the following discussion, that no loss of generality results when the f periods of pure process delay in Eq. 5 are absorbed into the B polynomial by including f leading zeros. Multiplying Eq. 5 (for $d = 1$) by $E_j(z^{-1})z^j$, substituting $E_j(z^{-1})A(z^{-1})\nabla$ from Eq. 22, and simplifying gives:

$$\hat{Y}_{t+j} = F_j(z^{-1})Y_t^f + G_j(z^{-1})\nabla U_{t+j-1}^f + E_j(z^{-1})a_{t+j} \tag{23}$$

where $G_j(z^{-1}) = E_j(z^{-1})B(z^{-1})$, and superscript f denotes filtering by $1/C(z^{-1})$. $E_j(z^{-1})$ is of degree $j - 1$ and, therefore, the final term in Eq. 23 involves only future unknown errors. After eliminating this term, the optimal predictor is given by:

$$\hat{Y}_{t+j} = F_j(z^{-1})Y_t^f + G_j(z^{-1})\nabla U_{t+j-1}^f \tag{24}$$

Minimization of the cost function, Eq. 21, is in terms of ∇U_t, not ∇U_t^f. Therefore, the prediction equation must be modified to separate past known filtered control actions from present and future unfiltered control actions yet to be determined. Consider the following identity:

$$G_j(z^{-1}) = G_j'(z^{-1})C(z^{-1}) + z^{-j}\Gamma_j(z^{-1}) \tag{25}$$

Substituting Eq. 25 into Eq. 24 gives:

$$\hat{Y}_{t+j} = F_j(z^{-1})Y_t^f + G_j'(z^{-1})\nabla U_{t+j-1} + \Gamma_j(z^{-1})\nabla U_{t-1}^f \tag{26}$$

The polynomials F_j, G_j' and Γ_j may be uniquely determined from

the system polynomials A, B, and C by the efficient recursion equations discussed by Clarke et al. (1987a,b). Substitution of Eq. 26 into the cost function, Eq. 21, and carrying out the minimization as in Clarke et al. (1987a) gives the control law:

$$\begin{bmatrix} \nabla U_t \\ \nabla U_{t+1} \\ \vdots \\ \nabla U_{t+NU-1} \end{bmatrix} = [H^T H + \rho I]^{-1} H^T \cdot \begin{bmatrix} W_{t+N1} - F_{N1} Y_t^f - \Gamma_{N1} \nabla U_{t-1}^f \\ W_{t+N1+1} - F_{N1+1} Y_t^f - \Gamma_{N1+1} \nabla U_{t-1}^f \\ \vdots \\ W_{t+N2} - F_{N2} Y_t^f - \Gamma_{N2} \nabla U_{t-1}^f \end{bmatrix} \quad (27)$$

where H is a matrix of dimension $(N2 - N1 + 1) \times (NU)$ composed of parameters in the polynomial G'_{N2}:

$$H = \begin{bmatrix} g'_{N1-1} & \cdots & g'_0 & 0 \\ & & & \\ \vdots & & & g'_0 \\ & & & \vdots \\ g'_{N2-1} & & \cdots & g'_{N2-NU} \end{bmatrix} \quad (28)$$

The four parameters $N1$, $N2$, NU, and ρ must be specified in order to achieve the desired closed-loop behavior. Note that no loss of generality results from assuming $N1 = 1$. Consider the special case when $NU = 1$. In this case the matrix H is a column vector and the term $H^T H + \rho I$ is a scalar, that is, a matrix inversion is avoided. This makes the algorithm much less computationally intensive, while maintaining many of the desirable properties of predictive control. An investigation of several different ways of choosing $N2$ and ρ is given by Allison et al. (1989). In the final analysis we chose the simplest approach; we omit the input weighting ($\rho = 0$) and use the output horizon ($N2$) as a tuning parameter. Note that increasing the output horizon $N2$ detunes the control.

Application to the Digester

Figure 9 is a block diagram of the adaptive GPC control strategy. Note that only the PID block in Figure 2 has been replaced. The production rate feedforward controller and the proportional-only feedback for high motor load remain.

Figure 10 shows a two-day period of digester operation producing grade K pulp. This is a continuation of the data shown in Figure 3. Results obtained from the closed-loop identification experiment were used to initialize the B polynomial parameters ($b_0 = -0.076$, $b_1 = 0.0$, and $b_2 = 0.0$). The output horizon ($N2$) was initially set equal to 20 control intervals (100 min). A long output horizon was used initially because operating personnel stressed the importance of minimizing blow flow manipula-

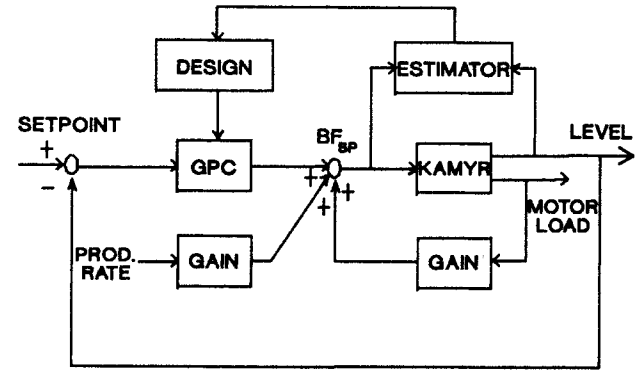

Figure 9. Adaptive chip level control strategy.

tions. Despite the detuning, the first ten or so hours of operation showed some oscillation in the level, indicating that the initial process gain estimate must have been too low, or the deadtime estimate too short. Nevertheless, the controller started to correct the problem right away. The parameter estimates all increase in absolute value to correct the gain and deadtime estimates. This eliminates the oscillation. At $t = 5$ h, the output horizon was decreased to 90 min ($N2 = 18$) and a further decrease to 75 min ($N2 = 15$) was made. Note the fast transition in the parameter

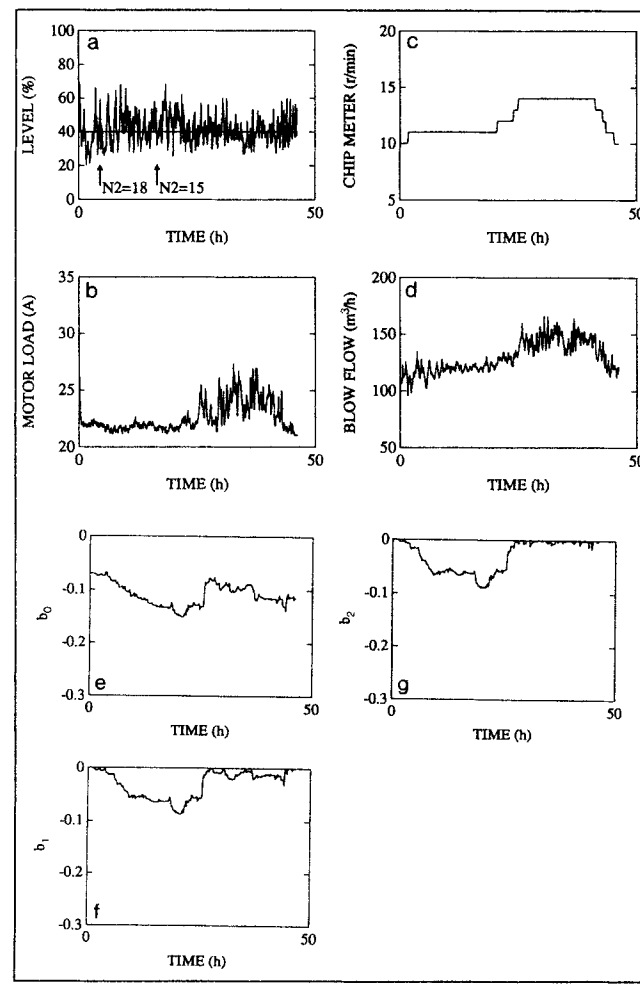

Figure 10. Start-up of adaptive controller.

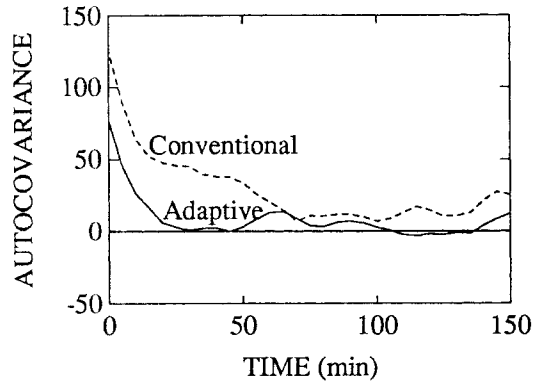

Figure 11. Autocovariance of level signal under conventional and adaptive control.

estimates during the production rate change at $t = 25$ h. The process gain and deadtime appear to be a strong function of the production rate, and the adaptive controller is able to compensate for these changes.

The adaptive controller provides some improvement in chip level control, despite large constraints on the blow flow manipulations. The adaptive controller follows the target value of 40% more closely, as indicated by the mean value of the level signal over the two-day test period. A mean value of 45.9% was achieved under conventional control, Figure 3, and 41.4% under adaptive control, Figure 10. Furthermore, the adaptive controller reduced the standard deviation of the chip level signal from 11.3 to 8.6% over the same period. This is illustrated in Figure 11, which shows the autocovariance of the level signal under conventional and adaptive control. Under adaptive control, the chip level signal is essentially uncorrelated beyond lag 3 (15 min.).

Figure 12 shows more than a full week of adaptive control while the digester was producing grade R pulp. Despite the frequent production rate changes, the operators only had to go to manual control on one occasion. Note that parameter b_0 generally tends to decrease in absolute value with decreases in production rate. This is opposite to the trend observed in Figure 10, suggesting that the process dynamics cannot be determined simply by knowing the production rate. The range of b_0 values in Figure 12 indicates that the process undergoes at least a fourfold change in steady-state gain over this range of operating conditions. This is consistent with the findings of Fuchs and Smith (1971). The fact that parameter b_2 is close to zero most of the time indicates that the process delay is likely not as long as 20 min but rather is most likely somewhere between 10 and 15 min.

The extent of delignification is most often characterized by the amount of residual lignin in the pulp as determined by standard laboratory tests (i.e., permanganate [P] number). It has been suggested (Roche, 1988) that up to 50% of P-number variability may be attributed to chip level variability. Therefore, it is reasonable to expect that improvements in level control should lead to direct improvements in pulp quality. Table 1 shows P-number means and standard deviations under conventional and adaptive chip level control. The data were obtained from monthly reports taken from the mill's technical department. P-numbers were routinely taken from blow line samples collected once every two hours. Results for both grades are shown. Days involving a grade change were not included in the analysis. P-number data corresponding to conventional level control were collected during the month of August 1988, the period just prior to start-up of the adaptive controller. September 1988 was chosen as the period representative of P-number variability under adaptive chip level control. Note that there is some improvement in P-number variability under adaptive control. For both grades, the average P-numbers are closer to the target values and the standard deviations are reduced.

Based on our experience from this application, we discuss below some practical considerations that may be useful in other adaptive control applications.

Parameter Constraints. One advantage to using an explicit approach to adaptive control—one in which the process model is identified directly—is that the model parameters often have a physical interpretation. In this application, for example, we built

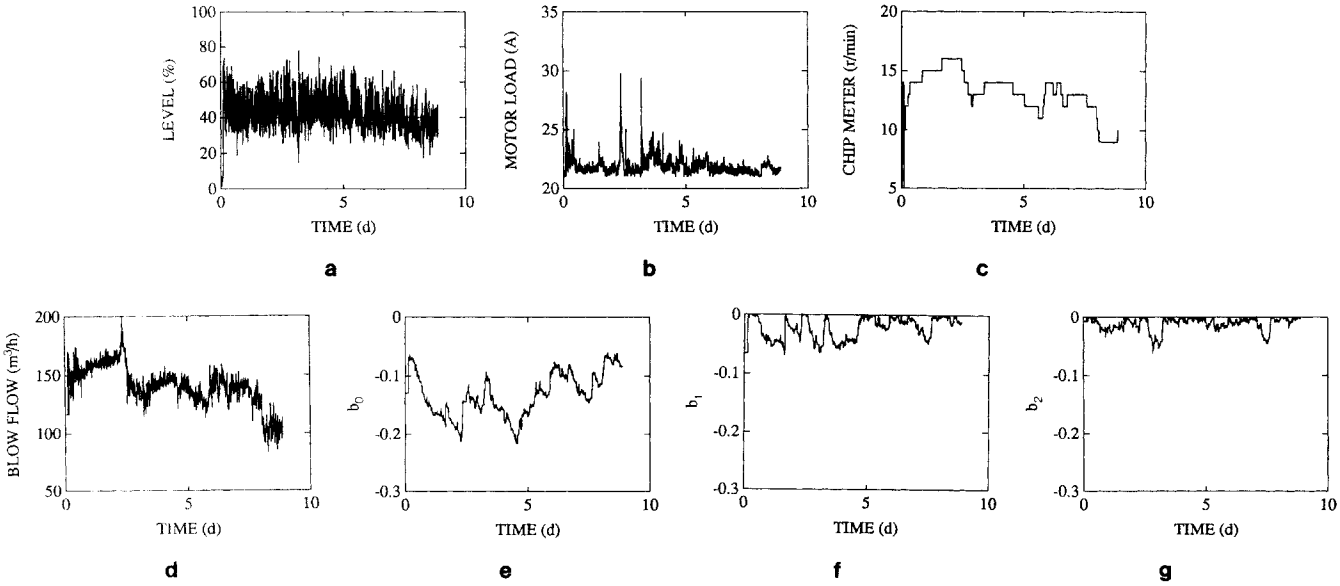

Figure 12. Nine days of adaptive chip level control, demonstrating operation under full range of production conditions.

Table 1. P-number Variability Under Conventional and Adaptive Chip Level Control Strategies

Chip Level Controller	Grade	Setpoint	Mean	Std. Dev.	No. Days Operation
Conventional	R	23.0	22.2	2.06	23
	K	21.0	19.9	1.91	6
Adaptive	R	23.0	22.4	1.76	18
	K	21.0	20.6	1.70	7

a significant amount of process knowledge into the estimator. We fixed a number of parameters (the time constant and noise model parameters) and only estimated the process gain within a well-defined range of possible time delays. Furthermore, the parameters that were estimated were only allowed to assume negative values because the process gain was known to be negative. Not all the parameter estimates were allowed to go to zero simultaneously because this would have resulted in excessive blow flow manipulation.

Estimator Enable/Disable. The chip level controller is left in adaptive mode except under the following circumstances:

1. auto/manual transfers
2. production rate changes
3. measurement saturation

The estimator is disabled when the controller is put into manual mode. On transfers from manual to automatic we wait five sampling intervals before switching the estimator back on. This minimizes any upset to the parameter estimates due to operator action. When the production rate changes, parameter estimation is disabled for five sampling intervals. Again, this avoids any large disturbances in the parameter estimates. The estimator is also disabled upon an extremely high or low chip level measurement because of strain gauge signal saturation. Note that when the estimator is disabled, the feedback controller still controls the chip level.

Controller Initialization. On transfer from manual to automatic it is necessary to initialize the feedback controller. This is often referred to as bumpless transfer. In order to prevent the controller from bumping the process on transfers to automatic, the operator will often preposition the blow flow setpoint. The bumpless transfer algorithm is designed to start control from this operator-entered blow flow. That is, if the chip level is equal to its setpoint on the transfer to automatic, the first blow flow manipulation will be zero.

Blow Flow Constraints. Absolute constraints are placed on the blow flow setpoint values coming from the chip level controller. These constraints are determined by the production rate. In adaptive control, one must be careful to provide the estimator with the constrained blow flow manipulations and not the unconstrained values coming directly from the feedback controller.

Although the adaptive controller has performed well since its commissioning in September 1988, it by no means has completely solved the problem of chip level control in Kamyr digesters. The measurements are still fairly crude and there are severe constraints on the amount of allowable blow flow manipulation, albeit for good reason. Nevertheless, the benefits that have been observed—reduced chip level and P-number variability, reduced need for operator intervention, and elimination of manual retuning—can be considered as incremental steps in the right direction. Hang-ups, however, are still a problem. Hang-ups occur when a portion of the chip column separates and plugs the digester. The problem may be alleviated by administering a shot of black liquor to the top of the digester, but by the time this is necessary a significant amount of production has already been lost and off-grade pulp produced. A more satisfactory solution would be to detect the situation at its onset in order to allow preventive measures to be taken. The adaptive chip level controller has demonstrated the potential for this type of advanced warning.

Figure 13 shows a period of operation leading up to a hang-up. Although the chip level is fairly well controlled right up until the hang-up causes a shutdown at $t = 25$ h, the parameter estimator appears to have identified a potential problem somewhere between the 10 and 15 h points. Apart from one short excursion, all three parameters hit and remained at their lower limits from the 15 h point onward. The estimator has picked up on the fact that the blow flow manipulations during this period of time are having much less than the normal effect on the chip level. This is what one expects to see when a portion of the column separates. This result appears to indicate that an early warning system for digester hang-up may be based on monitoring the adaptive controller's parameter estimates.

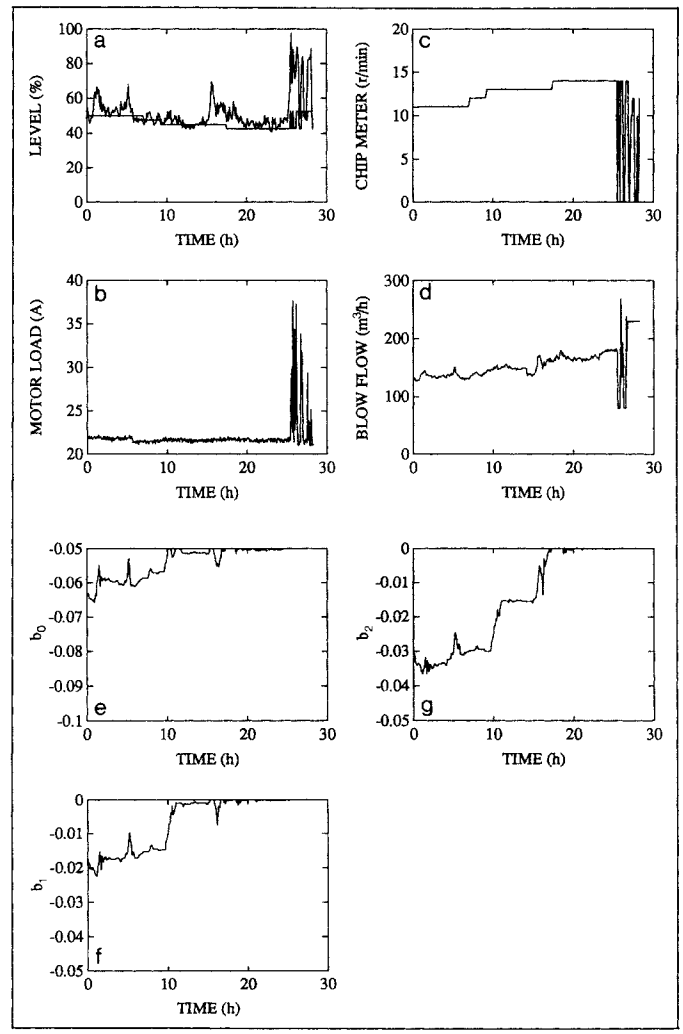

Figure 13. Parameter estimates during onset of a hang-up.

Conclusions

An adaptive chip level controller based on GPC has been successfully implemented on an industrial Kamyr digester. The model used in the design was experimentally identified from input/output data. A recursive identification algorithm estimates the model parameters on-line. The controller uses the model to predict the future behavior of the process output and to calculate the control actions required to minimize output deviations from target. The use of an explicit model allowed us to build a significant amount of process knowledge into the adaptive controller. The model parameters could be related to physically meaningful parts of the system and this was shown to be beneficial in detecting chip column hang-up. Other advantages of the adaptive control strategy include:

1. A reduction in chip level and P-number variability
2. Reduced need for operator intervention
3. Elimination of manual controller retuning

Acknowledgment

The authors gratefully acknowledge the Kamyr digester operators at Port Alberni for their cooperation and many helpful discussions. They also thank S. Ogawa for his assistance.

Notation

$A(z^{-1})$ = polynomial in combined model, Eq. 5
a = parameter in $A(z^{-1})$
a_t = white noise, Eq. 1
$B(z^{-1})$ = polynomial in combined model, Eq. 5
b = parameter in $B(z^{-1})$
$C(z^{-1})$ = polynomial in combined model, Eq. 5
c = parameter in $C(z^{-1})$
$E_j(z^{-1})$ = polynomial in Diophantine, Eq. 22
E = expectation
e = prediction error in RLS, Eq. 13
$F_j(z^{-1})$ = polynomial in Diophantine, Eq. 22
$G_j(z^{-1})$ = polynomial in output prediction, Eq. 23
$G'_j(z^{-1})$ = polynomial in modified output prediction, Eq. 26
g' = parameter in G'_j
H = matrix in GPC control law, Eq. 27
I = identify matrix, Eq. 27
J = quadratic cost function
k = lag in crosscovariance calculation, Eq. 2
K_c = proportional gain in PID controller, Eq. A7
K_1 = parameter in controller difference equation, Eq. A3
K_2 = parameter in controller difference equation, Eq. A3
K_3 = parameter in controller difference equation, Eq. A3
N = stochastic disturbance variable, Eq. 1
NU = control horizon, Eq. 21
$N1$ = minimum output horizon, Eq. 21
$N2$ = maximum output horizon, Eq. 21
P = covariance matrix in RLS, Eq. 14
$R(z^{-1})$ = denominator polynomial in controller transfer function, Eq. A1
r = parameter in $R(z^{-1})$
$S(z^{-1})$ = numerator polynomial in controller transfer function, Eq. A1
s = parameter in $S(z^{-1})$
U = manipulated variable (process input)
Y = controlled variable (process output)
T = sampling and control interval
T_d = derivative time in PID controller, Eq. A7
T_r = reset time in PID controller, Eq. A7
W = setpoint

Greek letters

α = parameter in RLS, Eq. 14
β = parameter in RLS, Eq. 15
$\Gamma_j(z^{-1})$ = polynomial in modified output prediction, Eq. 26
γ = crosscovariance, Eq. 2
$\delta(z^{-1})$ = denominator polynomial in process transfer function, Eq. 1
δ_1 = parameter in $\delta(z^{-1})$
η = parameter in intermediate calculation of bounds for P, Eq. 19
$\theta(z^{-1})$ = numerator polynomial in ARIMA disturbance model, Eq. 1
θ_1 = parameter in $\theta(z^{-1})$
θ = parameter vector in RLS, Eq. 14
λ = forgetting factor in RLS, Eq. 15
ρ = constraining parameter in GPC, Eq. 21
τ = parameter in RLS, Eq. 15
$\phi(z^{-1})$ = denominator polynomial in ARIMA disturbance model, Eq. 1
ϕ = regressor vector in RLS, Eq. 14
$\omega(z^{-1})$ = numerator polynomial in process transfer function, Eq. 1
ω_0 = parameter in $\omega(z^{-1})$
∇ = differencing operator, $(1 - z^{-1})$
ν = process transfer function impulse weight

Superscripts

d = degree of disturbance model nonstationarity
f = value filtered by $1/C(z^{-1})$
T = matrix transpose

Subscripts

d = dither signal
f = number whole sampling periods of pure process delay
j = number of future control and output horizon sampling intervals
u = process input
y = process output
$\hat{}$ = estimate

Literature Cited

Allison, B. J., G. A. Dumont, L. H. Novak, and W. J. Cheetham, "Adaptive-Predictive Control of Kamyr Digester Chip Level Using Strain Gauge Level Measurements," Pulp and Paper Rept. 739, Pulp and Paper Res. Inst. of Canada, Pointe Claire, Quebec (1989).

Åström, K. J., and B. Wittenmark, *Adaptive Control,* Addison-Wesley, Reading, MA (1989).

Bélanger, P. R., L. Rochon, G. A. Dumont, and S. Gendron, "Self-tuning Control of Chip Level in a Kamyr Digester," *AIChE J.*, **32**(1), 65 (1986).

Bergh, L. G., and J. F. MacGregor, "Constrained Minimum Variance Controllers: Internal Model Structure and Robustness Properties," *Ind. Eng. Chem. Res.*, **26**(8), 1558 (1987).

Box, G. E. P., and G. M. Jenkins, *Time Series Analysis; Forecasting and Control,* Holden-Day, San Francisco (1976).

Box, G. E. P., and J. F. MacGregor, "The Analysis of Closed-Loop Dynamic-Stochastic Systems," *Technometrics,* **10**(3), 391 (1974).

Cegrell, T., and T. Hedqvist, "A New Approach to Continuous Digester Control," *4th IFAC/IFIP Int. Conf. Digital Comp. Appl. to Process Control,* Zurich, 300 (1974).

Clarke, D. W., and P. J. Gawthrop, "Self-tuning Controller," *Proc. IEE,* **122,** 929 (1975).

Clarke, D. W., C. Mohtadi, and P. S. Tuffs, "Generalized Predictive Control. I: The Basic Algorithm," *Automatica,* **23**(2), 137 (1987a).

———, "Generalized Predictive Control. II: Extensions and Interpretations," *Automatica,* **23**(2), 149 (1987b).

Cohen, E. M., and T. L. Ryan, "Continuous Digester Level Control Using Discrete Level Indication," *TAPPI Alkaline Pulping Conf.*, Seattle, 91 (1974).

Dumont, G. A., "Applications of Advanced Control Methods in the Pulp and Paper Industry—A Survey," *Automatica,* **22**(2), 143 (1986).

Fortescue, T. R., L. S. Kershenbaum, and B. E. Ydstie, "Implementation of Self-tuning Regulators with Variable Forgetting Factors," *Automatica,* **17**(6), 831 (1981).

Fuchs, R. E., and C. L. Smith, "Blow Flow Control of Continuous Digesters," *TAPPI J.*, **54**(3), 368 (1971).

Harris, T. J., J. F. MacGregor, and J. D. Wright, "An Application of Self-tuning Regulators to Catalytic Reactor Control," *Joint Auto. Control Conf.*, Philadelphia (Oct., 1978).

———, "An Overview of Discrete Stochastic Controllers: Generalized PID Algorithms with Dead-Time Compensation," *Canad. J. Chem. Eng.*, **60**, 425 (1982).
Irving, E., "Improving Power Network Stability and Unit Stress with Adaptive Generator Control," *Automatica*, **15**, 31 (1979).
Lindqvist, S. O., "State of the Art in Continuous Digester Control," *Proc. EUCEPA Symp. Control Sys. in Pulp and Paper Industry*, Stockholm, 99 (1982).
McIntosh, A. R., S. L. Shah, and D. G. Fisher, "Experimental Evaluation of Adaptive Control in the Presence of Disturbances and Model-Plant Mismatch," *Workshop on Adaptive Control Strategies for Industrial Use*, Kananaskis, Alberta (June, 1988).
Roche, A., Unpublished results, Pulp and Paper Res. Inst. of Canada, Pointe Claire, Quebec (1988).
Salgado, M. E., G. C. Goodwin, and R. H. Middleton, "Modified Least-Squares Algorithm Incorporating Exponential Resetting and Forgetting," *Int. J. Control*, **47**(2), 477 (1988).
Sastry, V. A., "Self-tuning Control of Kamyr Digester Chip Level," *Pulp and Paper Canada*, **74**, T160 (1978).
Vroom, K. E., "The H Factor: A Means of Expressing Cooking Times and Temperatures as a Single Variable," *Pulp and Paper Canada*, **58**(3), 228 (1957).
Wittenmark, B., and K. J. Åström, "Practical Issues in the Implementation of Self-tuning Control," *Automatica*, **20**(5), 595 (1984).
Wong, P. M., P. A. Taylor, and J. D. Wright, "An Experimental Evaluation of Saturation Algorithms for Advanced Digital Controllers," *Ind. Eng. Chem. Res.*, **26**, 1117 (1987).

Appendix: Integral Action in Digital Controllers

Discrete digital controllers may always be written in the polynomial form:

$$\nabla U_t = \frac{S(z^{-1})}{R(z^{-1})}(W_t - Y_t) \tag{A1}$$

or, in expanded form:

$$\nabla U_t = [-(r_1 z^{-1} + r_2 z^{-2} + \cdots)\nabla U_t + (s_0 + s_1 z^{-1} + s_2 z^{-2} + \cdots)(W_t - Y_t)]/r_0 \tag{A2}$$

McIntosh et al. (1988) show how GPC may be put in the form of Eq. A1. Harris et al. (1982) show that Eq. A2 contains a discrete PID algorithm by multiplying through by the operator ∇^{-1} and rearranging to give:

$$U_t = -(r_1 U_{t-1} + r_2 U_{t-2} + \cdots)/r_0 + K_1(W_t - Y_t) + K_2 \sum_{i=0}^{\infty} (W_t - Y_{t-i}) + K_3 \nabla (W_t - Y_t) + \cdots \tag{A3}$$

In addition to the PID terms (terms involving K_1, K_2, and K_3), the discrete digital controller contains terms involving past control actions. These terms arise mainly from the presence of process deadtime and amount to deadtime compensation terms in the controller.

The numerator polynomial $S(z^{-1})$ in Eq. A1 for GPC and the identified process model, Eq. 3, is a function of the transfer function denominator $\delta(z^{-1})$ and the numerator of the optimal disturbance forecast $(1 - \theta)$ (Harris et al., 1982); that is, the controller zeros are not affected by the tuning parameters. Therefore, $S(z^{-1})$ in this case is given by:

$$S(z^{-1}) = (1 - \theta)(1 - \delta_1 z^{-1}) \tag{A4}$$

Wong et al. (1987) show that the following relationships hold where K_1 and K_2 are the proportional and integral gains, respectively, from Eq. A3:

$$K_1 = -s_1/r_0$$
$$K_2 = s_0/r_0 - K_1 \tag{A5}$$

Upon substitution of Eq. A4 into Eq. A5 we get:

$$K_1 = (1 - \theta)\delta_1/r_0$$
$$K_2 = (1 - \theta)(1 - \delta_1)/r_0 \tag{A6}$$

The standard form of the discrete PID controller may be written as:

$$U_t = K_c\left[(W_t - Y_t) + T/T_r \sum_{i=0}^{\infty} (W_t - Y_{t-i}) + T_d/T\,\nabla(W_t - Y_t)\right] \tag{A7}$$

Equating coefficients in Eqs. A3 and A7 gives:

$$K_1 = K_c$$
$$K_2 = K_c T/T_r \tag{A8}$$

Upon substitution of Eq. A6 into Eq. A8 we obtain the following expression for the reset time T_r:

$$T_r = \frac{\delta_1}{1 - \delta_1} T \tag{A9}$$

Manuscript received Jan. 22, 1990, and revision received May 18, 1990.